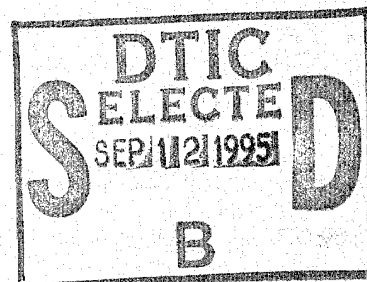


# Analysis of the Page Test With Nuisance Parameter Estimation for Various Signal Types

Douglas A. Abraham  
Submarine Sonar Department



**Naval Undersea Warfare Center Division**  
**Newport, Rhode Island**

Approved for public release; distribution is unlimited.

DTIC QUALITY INSPECTED 8

19950911 064

## PREFACE

The work presented in this report was sponsored by the Naval Undersea Warfare Center's (NUWC's) Independent Research (IR) Program, as Project B10001, entitled *Quickest Detection of Signals in the Presence of Noise With Unknown Parameters*. The IR Program is funded by the Office of Naval Research; the NUWC program manager was Dr. Kenneth M. Lima (Code 102).

The technical reviewer for this report was S. Greineder (Code 2121). The author wishes to thank Dr. A. Nuttall (Code 302) for his help with contour integration.

**Reviewed and Approved:** 22 May 1995

A handwritten signature in black ink, appearing to read 'R. J. Martin', written in a cursive style.

**R. J. Martin**  
**Head, Submarine Sonar Department**  
*(acting)*

# REPORT DOCUMENTATION PAGE

*Form Approved*  
OMB No. 0704-0188

Public reporting burden for this collection of information is estimated to average 1 hour per response, including the time for reviewing instructions, searching existing data sources, gathering and maintaining the data needed, and completing and reviewing the collection of information. Send comments regarding this burden estimate or any other aspect of this collection of information, including suggestions for reducing this burden, to Washington Headquarters Services, Directorate for Information Operations and Reports, 1215 Jefferson Davis Highway, Suite 1204, Arlington, VA 22202-4302, and to the Office of Management and Budget, Paperwork Reduction Project (0704-0188), Washington, DC 20503.

1. AGENCY USE ONLY (Leave Blank)	2. REPORT DATE <p style="text-align: center;">22 May 1995</p>	3. REPORT TYPE AND DATES COVERED <p style="text-align: center;">Final</p>	
4. TITLE AND SUBTITLE <p style="text-align: center;"><b>Analysis of the Page Test With Nuisance Parameter Estimation for Various Signal Types</b></p>		5. FUNDING NUMBERS	
6. AUTHOR(S) <p style="text-align: center;">Douglas A. Abraham</p>		8. PERFORMING ORGANIZATION REPORT NUMBER <p style="text-align: center;">TR 10,991</p>	
7. PERFORMING ORGANIZATION NAME(S) AND ADDRESS(ES) <p style="text-align: center;">Naval Undersea Warfare Center Detachment New London New London, Connecticut 06320</p>			
9. SPONSORING/MONITORING AGENCY NAME(S) AND ADDRESS(ES) <p style="text-align: center;">Office of Naval Research 800 North Quincy Street Arlington, VA 22217-5000</p>			
11. SUPPLEMENTARY NOTES			
12a. DISTRIBUTION/AVAILABILITY STATEMENT <p style="text-align: center;">Approved for public release; distribution is unlimited.</p>		12b. DISTRIBUTION CODE	
13. ABSTRACT (Maximum 200 words) <p>The Page test with nuisance parameter estimation is applied to the detection of the following signal types: (i) complex Gaussian distributed data with a shift in mean signal and unknown variance, (ii) exponentially distributed data with an unknown noise power, and (iii) multivariate complex Gaussian distributed data with a deterministic array signal and an unknown interference covariance matrix.</p> <p>For each signal type, a detector nonlinearity is developed and the Siegmund-based approximations to the average sample number derived. Comparison to simulation indicates that the Siegmund-based approximations are more accurate than the Wald-based approximations and that there is a sensitivity to corruption of the auxiliary data by signal-presence when the buffer size is inadequate at low signal-to-noise ratios. Operating characteristic curves for each of the signal types are generated describing the performance of the detectors as a function of threshold and SNR.</p> <p>The probability of detecting a finite duration signal is approximated by the Brownian motion and moment matching approximation of [Han et al.] and estimated by the Poisson mixture method of [Abraham] where it was observed that the Poisson mixture method provided the least total estimation error.</p> <p>Nonparametric signal-onset detection is discussed within the framework of the Page test with nuisance parameter estimation.</p>			
14. SUBJECT TERMS page test average sample number		nuisance parameter nonparametric detection	
		15. NUMBER OF PAGES <p style="text-align: center;">52</p>	16. PRICE CODE
17. SECURITY CLASSIFICATION OF REPORT <p style="text-align: center;"><b>UNCLASSIFIED</b></p>	18. SECURITY CLASSIFICATION OF THIS PAGE <p style="text-align: center;"><b>UNCLASSIFIED</b></p>	19. SECURITY CLASSIFICATION OF ABSTRACT <p style="text-align: center;"><b>UNCLASSIFIED</b></p>	20. LIMITATION OF ABSTRACT <p style="text-align: center;"><b>SAR</b></p>

## TABLE OF CONTENTS

	Page
LIST OF ILLUSTRATIONS . . . . .	ii
LIST OF SYMBOLS . . . . .	iv
LIST OF ACRONYMS . . . . .	v
INTRODUCTION . . . . .	1
COMPLEX GAUSSIAN SHIFT IN MEAN SIGNAL WITH UNKNOWN VARIANCE	2
STATISTICAL DESCRIPTION . . . . .	2
DETECTOR NONLINEARITY . . . . .	2
EXPECTATIONS OVER NUISANCE PARAMETER ESTIMATE . . . . .	4
AVERAGE SAMPLE NUMBER AND DETECTION PROBABILITY ANALYSIS	7
EXPONENTIAL SIGNAL WITH UNKNOWN NOISE POWER . . . . .	14
STATISTICAL DESCRIPTION . . . . .	14
DETECTOR NONLINEARITY . . . . .	14
EXPECTATIONS OVER NUISANCE PARAMETER ESTIMATE . . . . .	16
AVERAGE SAMPLE NUMBER AND DETECTION PROBABILITY ANALYSIS	17
MULTIVARIATE COMPLEX GAUSSIAN DETERMINISTIC SIGNAL WITH UN- KNOWN INTERFERENCE COVARIANCE MATRIX . . . . .	24
STATISTICAL DESCRIPTION . . . . .	24
DETECTOR NONLINEARITY . . . . .	24
EXPECTATIONS OVER NUISANCE PARAMETER ESTIMATE . . . . .	27
AVERAGE SAMPLE NUMBER ANALYSIS . . . . .	29
NONPARAMETRIC CHANGE DETECTION . . . . .	33
CONCLUSIONS . . . . .	35
REFERENCES . . . . .	37
APPENDIX A: MGF UNITY ROOT FOR A NONCENTRAL CHI-SQUARED RAN- DOM VARIABLE . . . . .	A-1
APPENDIX B: MGF UNITY ROOT FOR AN EXPONENTIAL RANDOM VARI- ABLE . . . . .	B-1

LIST OF ILLUSTRATIONS

Figure		Page
1	Average Delay Before Detection Vs. Average Time Between False Alarms for 0 dB SNR and Varying Amounts of Auxiliary Data . . . . .	10
2	Average Time Between False Alarms Vs. Threshold for Varying Amounts of Auxiliary Data . . . . .	11
3	Average Delay Before Detection Vs. SNR for $\bar{T} = 10^3$ Samples and Varying Amounts of Auxiliary Data . . . . .	11
4	Simulation and Siegmund- and Wald-Based Approximations to Average Time Between False Alarms Vs. Threshold for $J = 30$ . . . . .	12
5	Simulation and Siegmund- and Wald-Based Approximations to Average Delay Before Detection Vs. SNR for $J = 30$ and $\bar{T} = 10^3$ Samples . . . . .	12
6	Approximations to the Probability of Detection Vs. Signal Duration for 0 dB and 5 dB SNR, $J = 30$ , and $\bar{T} = 10^3$ Samples . . . . .	13
7	Total Error Between Sample CDF and Probability of Detection Approximations Vs. SNR for $J = 30$ and $\bar{T} = 10^3$ Samples . . . . .	13
8	Average Delay Before Detection Vs. Average Time Between False Alarms for 0 dB SNR, and Varying Amounts of Auxiliary Data . . . . .	20
9	Average Time Between False Alarms Vs. Threshold for Varying Amounts of Auxiliary Data . . . . .	21
10	Average Delay Before Detection Vs. SNR for $\bar{T} = 10^3$ Samples and Varying Amounts of Auxiliary Data . . . . .	21
11	Simulation and Siegmund- and Wald-Based Approximations to Average Time Between False Alarms Vs. Threshold for $J = 30$ . . . . .	22
12	Simulation and Siegmund- and Wald-Based Approximations to Average Delay Before Detection Vs. SNR for $J = 30$ and $\bar{T} = 10^3$ Samples . . . . .	22
13	Approximations to the Probability of Detection Vs. Signal Duration for 0 dB and 5 dB SNR, $J = 30$ , and $\bar{T} = 10^3$ Samples . . . . .	23
14	Total Error Between Sample CDF and Probability of Detection Approximations Vs. SNR for $J = 30$ and $\bar{T} = 10^3$ Samples . . . . .	23
15	Simulation and Siegmund-Based Approximation to Average Time Between False Alarms Vs. Threshold for $N = 5$ and $J = 30$ . . . . .	31
16	Simulation and Siegmund-Based Approximation to Average Delay Before Detection Vs. Threshold for $N = 5$ , $J = 30$ , and 0 dB SNR . . . . .	31

17 Average Time Between False Alarms Vs. Threshold for 0 dB SNR,  $N = 5$ , and Varying Amounts of Auxiliary Data . . . . . 32

18 Average Delay Before Detection Vs. Threshold for 0 dB SNR,  $N = 5$ , and Varying Amounts of Auxiliary Data . . . . . 32

A-1 Possible Configurations of  $\phi(t)$  for Noncentral Chi-squared Random Variable A-3

Accession For	
DTIC GRA&I	<input checked="" type="checkbox"/>
DTIC TAB	<input type="checkbox"/>
Unannounced	<input type="checkbox"/>
Justification	
By	
Distribution/	
Availability Codes	
Dist	Avail and/or Special
A-1	

## LIST OF SYMBOLS

$A_S(s)$	Siegmund-based approximation to the ASN for the Page test with nuisance parameter estimation
$A_S^\infty(s)$	Siegmund-based approximation to the ASN for Page test
$\mathbf{d}$	Array steering vector
$\bar{D}$	Average delay before detection for standard Page test
$\delta$	Noncentrality parameter for chi-squared distribution
$E_i(s)$	Expectations over nuisance parameter for ASN analysis
$h$	Detector threshold
$I(\gamma, \alpha, \beta)$	Intermediate function
$J$	Amount of auxiliary data
$p$	Beta random variable
$\phi(t)$	Natural logarithm of MGF
$r$	Gamma random variable
$\rho_-^\delta, \rho_-$	Siegmund correction term for excess below zero
$\rho_+^\delta, \rho_+$	Siegmund correction term for excess above $h$
$s$	Signal-to-noise or signal-to-interference ratio
$\bar{s}$	Design SNR or SIR parameter
$\sigma^2$	Noise variance
$\Sigma$	Interference covariance matrix
$\bar{T}$	Average time between false alarms for standard Page test
$\theta$	Signal strength parameter
$\bar{\theta}$	Design signal strength parameter

## LIST OF ACRONYMS

ASN	Average sample number
CDF	Cumulative distribution function
GLR	Generalized likelihood ratio
LLR	Log-likelihood ratio
LO	Locally optimal
MDL	Minimum detectable signal level
MGF	Moment generating function
MLE	Maximum likelihood estimate
OC	Operating characteristic
PDF	Probability density function
SIR	Signal-to-interference ratio
SNR	Signal-to-noise ratio

# ANALYSIS OF THE PAGE TEST WITH NUISANCE PARAMETER ESTIMATION FOR VARIOUS SIGNAL TYPES

## INTRODUCTION

In [1], the Page test with nuisance parameter estimation was introduced as a method for the detection of a change from signal-absence (hypothesis H) to signal-presence (hypothesis K) when the observed data are statistically characterized by a model having unknown noise parameters with the same value under both H and K. The real Gaussian shift in mean signal with unknown variance was considered in [1] as an example illustrating the accuracy of the Siegmund-based approximations to the average sample numbers (ASNs) for the Page test, the average delay before detection ( $\bar{D}$ ) and the average time between false alarms ( $\bar{T}$ ). In this report, the Page test with nuisance parameter estimation is applied to the following situations: (i) complex Gaussian distributed data with a shift in mean signal and unknown variance, (ii) exponentially distributed data with an unknown noise power, and (iii) multivariate complex Gaussian distributed data with a deterministic array signal and an unknown interference covariance matrix. In the following sections, the detector nonlinearity, ASN analysis, and performance evaluation of each of the above situations is developed and presented.

A more appropriate signal model in sonar consists of a signal that starts and then stops. The probability of detecting such a finite duration signal using the Page test with nuisance parameter estimation is approximated by the Brownian motion and moment matching approximations of [2] and estimated by the Poisson mixture method of [3].

The application of the Page test with nuisance parameter estimation to nonparametric change detection is also discussed.

## COMPLEX GAUSSIAN SHIFT IN MEAN SIGNAL WITH UNKNOWN VARIANCE

Complex Gaussian data are typically observed at the output of discrete Fourier transforms subject to Gaussian random process excitation or after basebanding operations. The complex shift in mean signal results from sinusoidal signals with unknown phase. In most realistic situations, the variance of the complex Gaussian data is unknown.

### STATISTICAL DESCRIPTION

The observed data are assumed to be distributed according to

$$x_i \sim \begin{cases} \mathcal{CN}(0, \sigma^2) & i < q \\ \mathcal{CN}(\mu, \sigma^2) & i \geq q \end{cases}, \quad (1)$$

where  $\sigma^2$  is the unknown variance of the observed data,  $\mu$  is the unknown complex mean of the signal, and  $q$  is the unknown starting time of the signal. The notation  $x \sim \mathcal{CN}(\mu, \sigma^2)$  indicates that the random variable  $x$  has a complex Gaussian distribution with mean  $\mu$ , variance  $\sigma^2$ , and probability density function (PDF)

$$f(x) = \frac{1}{\pi\sigma^2} e^{-\frac{|x-\mu|^2}{\sigma^2}}, \quad (2)$$

for  $x \in \mathcal{C}$ , where  $\mathcal{C}$  is the complex plane.

### DETECTOR NONLINEARITY

If the nuisance parameter, in this case  $\sigma^2$ , were known, the detector nonlinearity used in the Page test would be either a locally optimal (LO) or generalized likelihood ratio (GLR) nonlinearity. As the signal is represented here by a complex mean, direct application of the LO nonlinearity is not straightforward. However, the GLR nonlinearity may be easily derived by describing the log-likelihood ratio (LLR) as

$$l(x) = \log \frac{f_K(x)}{f_H(x)}$$

$$= \frac{|x|^2}{\sigma^2} - \frac{|x - \mu|^2}{\sigma^2} . \quad (3)$$

The GLR statistic is the maximum of the LLR over all possible values of the unknown complex signal amplitude  $\mu$ . Maximizing equation (3) clearly requires choosing  $\hat{\mu} = x$  which leads to the GLR statistic

$$T(x) = \frac{|x|^2}{\sigma^2} . \quad (4)$$

Utilization of this statistic in the Page test requires a bias to force the mean negative under hypothesis H and substitution of an estimate of the nuisance parameter. At this point it is useful to recognize that  $T(x)$  is the scale of a noncentral chi-squared random variable with two degrees of freedom, thus,

$$V = \frac{2|x|^2}{\sigma^2} \sim \mathcal{X}_2^2(\delta) , \quad (5)$$

where  $\delta = \frac{2|\mu|^2}{\sigma^2} = 2s$  is the noncentrality parameter ( $s = \frac{|\mu|^2}{\sigma^2}$ ). Thus, the bias may be chosen to maximize the asymptotic Page test performance for a *design* noncentrality parameter,  $\tilde{\delta}$ , as shown in [4]. Unfortunately, upon substitution of the nuisance parameter estimate, this leads to very cumbersome analysis. As described in [4], an alternative for weak signals is the Dyson bias, which has the form

$$\tau = n + \frac{\tilde{\delta}}{2} \quad (6)$$

for noncentral chi-squared signals with  $n$  degrees of freedom. Thus, upon use of the Dyson bias and substitution of the nuisance parameter estimate, the Page test nonlinearity has the form

$$g(x, \hat{\sigma}^2) = 2\frac{|x|^2}{\hat{\sigma}^2} - 2 - \frac{\tilde{a}}{\hat{\sigma}^2} \quad (7)$$

$$\begin{aligned} &= \frac{V}{\frac{\hat{\sigma}^2}{\sigma^2}} - 2 - \frac{\tilde{s}}{\frac{\hat{\sigma}^2}{\sigma^2}} \\ &= \frac{V}{r} - 2 - \frac{\tilde{s}}{r} , \end{aligned} \quad (8)$$

where  $r = \frac{\hat{\sigma}^2}{\sigma^2}$ ,  $\tilde{a} = |\tilde{\mu}|^2$  is a design signal power, and  $\tilde{s} = \frac{\tilde{a}}{\sigma^2}$  is a design signal-to-noise power ratio (SNR).

The ASN analysis requires the mean, moment-generating-function (MGF) unity root, and Siegmund correction terms of the detector nonlinearity (7) under hypotheses H and K conditioned on the observed nuisance parameter estimate  $\hat{\sigma}^2$ . The detector nonlinearity is a scaled and shifted noncentral chi-squared random variable under H and K. A numerical routine for obtaining the MGF unity root is presented in Appendix A. The conditional mean is

$$\begin{aligned} \mathbb{E} [g(x, \hat{\sigma}^2) | \hat{\sigma}^2] &= \frac{\mathbb{E}[V]}{r} - 2 - \frac{\tilde{s}}{r} \\ &= \frac{2 + \delta}{r} - 2 - \frac{\tilde{s}}{r} \\ &= \frac{2}{r} \left( 1 + s - \frac{\tilde{s}}{2} \right) - 2, \end{aligned} \quad (9)$$

where here and in the following, hypothesis H is obtained by setting  $\delta = s = 0$ . The Siegmund correction terms conditioned on  $\hat{\sigma}^2$  are

$$\rho_{\pm}^{\delta} = \frac{\rho_{\pm}^{\delta}}{r}, \quad (10)$$

where  $\rho_{\pm}^{\delta}$  are, as described in [1], the Siegmund correction terms for a noncentral chi-squared random variable with two degrees of freedom and noncentrality parameter  $\delta$ . As found in [1], the correction terms when no signal is present are  $\rho_{+}^0 = 2$  and  $\rho_{-}^0 = -\frac{2}{3}$ .

## EXPECTATIONS OVER NUISANCE PARAMETER ESTIMATE

As seen in [1], the Siegmund-based approximation to the ASN of the Page test with nuisance parameter estimation requires the expectation of three functions of the nuisance parameter estimate. They are described in this section for the complex Gaussian shift in mean signal. The nuisance parameter estimate is the maximum likelihood estimate (MLE) of the variance over the auxiliary data. If the auxiliary data  $(y_1, \dots, y_J)$  are independent and identically distributed according to

$$y_j \sim \mathcal{CN}(0, \sigma^2), \quad (11)$$

the nuisance parameter estimate has the form

$$\hat{\sigma}^2 = \frac{1}{J} \sum_{j=1}^J |y_j|^2. \quad (12)$$

Since  $\frac{2|y_j|^2}{\sigma^2} \sim \chi^2_2$  is centrally chi-squared distributed with two degrees of freedom,  $2J\frac{\hat{\sigma}^2}{\sigma^2} \sim \chi^2_{2J}$ . Thus,  $r$  follows a Gamma distribution

$$r = \frac{\hat{\sigma}^2}{\sigma^2} \sim \text{Gamma}\left(J, \frac{1}{J}\right), \quad (13)$$

which has PDF

$$f(r) = \frac{J^J r^{J-1} e^{-Jr}}{\Gamma(J)} \quad (14)$$

for  $r \geq 0$ .

The first expectation is

$$\begin{aligned} E_1(s) &= \text{E}\left[\frac{1}{\text{E}[g|\hat{\sigma}^2]}\right] \\ &= -\frac{1}{2} \text{E}\left[\frac{r}{r - \left(1 + s - \frac{\tilde{s}}{2}\right)}\right] \end{aligned} \quad (15)$$

$$= -\frac{1}{2} I\left(1 + s - \frac{\tilde{s}}{2}, J, \frac{1}{J}\right), \quad (16)$$

where, if  $r$  follows the gamma distribution with degrees of freedom parameter  $\alpha$  and scale parameter  $\beta$ , the expectation of equation (15) may be described by the general function

$$\begin{aligned} I(\gamma, \alpha, \beta) &= \text{E}\left[\frac{r}{r - \gamma}\right] \\ &= \int_{r=0}^{\infty} \left(\frac{r}{r - \gamma}\right) \frac{r^{\alpha-1} e^{-\frac{r}{\beta}}}{\Gamma(\alpha) \beta^\alpha} dr \end{aligned} \quad (17)$$

$$= \int_{r=0}^{\infty} \frac{\left(\frac{r}{\beta}\right)^\alpha e^{-\frac{r}{\beta}}}{\Gamma(\alpha) (r - \gamma)} dr, \quad (18)$$

with the notation  $\int$  representing the principal value integral. By moving the principal value integral of equation (18) from the real axis upward into the complex plane,  $I(\gamma, \alpha, \beta)$  may be described as

$$I(\gamma, \alpha, \beta) = \int_C f(z) dz + i\pi \text{Res}\{f(z); z = \gamma\} \quad (19)$$

where

$$f(z) = \frac{\left(\frac{z}{\beta}\right)^\alpha e^{-\frac{z}{\beta}}}{\Gamma(\alpha) (z - \gamma)}, \quad (20)$$

and  $C$  is any contour in the first quadrant from the origin to  $z = \infty$ . The residue of  $f(z)$  at  $z = \gamma$  is

$$\begin{aligned} \text{Res}\{f(z); z = \gamma\} &= [(z - \gamma)f(z)]|_{z=\gamma} \\ &= \frac{\left(\frac{\gamma}{\beta}\right)^\alpha e^{-\frac{\gamma}{\beta}}}{\Gamma(\alpha)}. \end{aligned} \quad (21)$$

The contour  $C$  may be described as the limit as  $A \rightarrow \infty$  of  $C_{\theta,A} \cup C_A$  where  $C_{\theta,A}$  is the integral from the origin to the point  $Ae^{j\theta}$  and  $C_A$  is the integral along the arc of radius  $A$  from angle  $\theta$  to angle zero. Due to the exponential term in  $f(z)$ , this latter integral goes to zero as  $A \rightarrow \infty$ . Thus, letting  $z = ae^{j\theta}$  ( $dz = e^{j\theta} da$ ) results in

$$\begin{aligned} \int_C f(z) dz &= \int_{C_{\theta,\infty}} f(z) dz \\ &= e^{j\theta} \int_{a=0}^{\infty} f(ae^{j\theta}) da, \end{aligned} \quad (22)$$

which, when  $\theta$  is appropriately chosen, may be easily performed numerically. Due to the  $e^{-\frac{z}{\beta}}$  term in  $f(z)$ , the substitution  $z = ae^{j\theta}$  results in the sinusoidal term  $e^{-ja\frac{\sin(\theta)}{\beta}}$ . This function causes problems in numerical integration routines when  $\beta$  is small. Thus, it is suggested that  $\theta$  be chosen proportional to  $\beta$  to keep the frequency of the sinusoidal terms approximately constant as  $\beta$  varies. Choosing  $\theta = \frac{10\pi\beta}{3}$  was observed to work well for  $\beta$  between 0.1 ( $J = 10$ ) and 0.01 ( $J = 100$ ).

It should be noted that  $I(\gamma, \alpha, \beta)$  may be computed recursively if  $\alpha$  is an integer with an initial starting value requiring evaluation of the exponential integral. However, the recursion is unstable for large values of  $\alpha$  (i.e.,  $\alpha = J > 30$ ).

The second expectation is

$$\begin{aligned} E_2^\pm(s) &= E\left[\frac{\rho_\pm}{E[g|\hat{\sigma}^2]}\right] \\ &= -\frac{\rho_\pm^\delta}{2} E\left[\frac{1}{r - \left(1 + s - \frac{s}{2}\right)}\right]. \end{aligned} \quad (23)$$

Now, observe that equation (17) may be written as

$$I(\gamma, \alpha, \beta) = \int_{r=0}^{\infty} \frac{(r - \gamma + \gamma) r^{\alpha-1} e^{-\frac{r}{\beta}}}{\Gamma(\alpha) \beta^\alpha (r - \gamma)} dr$$

$$\begin{aligned}
&= \int_{r=0}^{\infty} \frac{r^{\alpha-1} e^{-\frac{r}{\beta}}}{\Gamma(\alpha) \beta^{\alpha}} dr + \gamma \int_{r=0}^{\infty} \frac{r^{\alpha-1} e^{-\frac{r}{\beta}}}{\Gamma(\alpha) \beta^{\alpha} (r-\gamma)} dr \\
&= 1 + \gamma E \left[ \frac{1}{r-\gamma} \right], \tag{24}
\end{aligned}$$

where the first integral in the second line is recognized as the integral of the PDF of  $r$ . Thus,

$$E \left[ \frac{1}{r-\gamma} \right] = \frac{I(\gamma, \alpha, \beta) - 1}{\gamma} \tag{25}$$

and

$$E_2^{\pm}(s) = -\frac{\rho_{\pm}^{\delta}}{2 \left(1 + s - \frac{\tilde{s}}{2}\right)} \left[ I \left( 1 + s - \frac{\tilde{s}}{2}, J, \frac{1}{J} \right) - 1 \right]. \tag{26}$$

The third expectation has the form

$$\begin{aligned}
E_3(s) &= E \left[ \frac{t_s \rho_-}{1 - e^{t_s(h+\rho_+ - \rho_-)}} \right] \\
&= \rho_-^{\delta} E \left[ \frac{r^{-1} t_s}{1 - e^{t_s(h+r^{-1}(\rho_+^{\delta} - \rho_-^{\delta}))}} \right] \\
&= \rho_-^{\delta} \int_{r=0}^{\infty} \frac{r^{-1} t_s}{1 - e^{t_s(h+r^{-1}(\rho_+^{\delta} - \rho_-^{\delta}))}} f(r) dr, \tag{27}
\end{aligned}$$

where  $t_s$  is the MGF unity root of the Page test update when  $\delta = 2s$  is the noncentrality parameter and the scale and bias terms are as found in equation (8). This expectation is easily performed by standard numerical integration with  $t_s$  obtained as a function of the variables  $(s, \tilde{s}, r)$  using the method described in Appendix A.

## AVERAGE SAMPLE NUMBER AND DETECTION PROBABILITY ANALYSIS

Combining equations (16), (26), and (27) as described in [1] results in the Siegmund-based approximation

$$\begin{aligned}
A_S(s) &= hE_1(s) + E_2^+(s) - E_2^-(s) + \frac{E_2^-(s)}{E_3(s)} \\
&= \frac{-h}{2} I \left( \gamma, J, \frac{1}{J} \right) - \frac{(\rho_+^{\delta} - \rho_-^{\delta})}{2\gamma} \left[ I \left( \gamma, J, \frac{1}{J} \right) - 1 \right] - \frac{\rho_-^{\delta} \left[ I \left( \gamma, J, \frac{1}{J} \right) - 1 \right]}{2\gamma E_3(s)}, \tag{28}
\end{aligned}$$

where  $\gamma = 1 + s - \frac{\tilde{s}}{2}$ . The average time between false alarms is obtained when  $\delta = s = 0$ .

When the nuisance parameter is perfectly estimated (i.e.,  $J \rightarrow \infty$ ),  $r \rightarrow 1$  and the Page test with nuisance parameter estimation results in the standard Page test. In this case, the Siegmund-based approximation to the ASN is

$$A_S^\infty(s) = \frac{1 + t_s h_s - e^{t_s h_s}}{2t_s \left(s - \frac{\tilde{s}}{2}\right)}, \quad (29)$$

where  $h_s = h + \rho_+^\delta - \rho_-^\delta$  and  $t_s$  is, as before, the MGF unity root where  $r = 1$  in the scale and bias terms of equation (8).

The above Siegmund-based approximations to the average time between false alarms ( $\delta = s = 0$ ) and the average delay before detection ( $\delta = 2s > 0$ ) are used to evaluate the performance of the Page test with nuisance parameter estimation for the complex Gaussian shift in mean signal. Figure 1 contains the Page test operating characteristic (OC) curve for  $s = 0$  dB, a design SNR  $\tilde{s} = 0$  dB, and for auxiliary data amounts  $J = 10, 20, 30, 50, 100$ , and  $\infty$  (perfect estimation of the nuisance parameter). Curves of the average time between false alarms as a function of the threshold for the above situation are found in figure 2. The average delay before detection as a function of SNR is found in figure 3 where the design SNR and average time between false alarms are held constant at  $\tilde{s} = 0$  dB and  $\bar{T} = 10^3$ , respectively. The signal level that produces a zero mean in the Page test update, and therefore a very large average delay before detection, is considered the minimum detectable signal level (MDL). In this situation the MDL increases as  $J$  decreases from approximately  $-3$  dB for  $J = \infty$ .

Simulations are performed to validate the approximations to  $\bar{T}$  and  $\bar{D}$  and to evaluate the performance of existing methods for approximating the probability of detecting a finite-duration signal using the Page test with nuisance parameter estimation. Figures 4 and 5 contain the Siegmund- and Wald-based approximations to  $\bar{T}$  and  $\bar{D}$  along with that estimated from simulation. As seen in [1], the Wald-based approximations may be obtained from  $E_1(s)$  and from  $E_3(s)$  with a slight modification. As the Siegmund-based approximations are more accurate than the Wald-based ones, this modification is left to those interested in analyzing the Wald-based approximations. In all cases, the design SNR is 0 dB and  $J = 30$  samples of auxiliary data are used to estimate the nuisance parameter with a 60 sample buffer. The thresholds for the results shown in figure 5 are set according to  $\bar{T} = 10^3$ . The discrepancy

between the Siegmund-based approximation to  $\bar{D}$  and the simulations at lower SNR is the result of an inadequate buffer size. In this situation, the nuisance parameter estimate is corrupted by data containing signal, particularly for SNRs below 1.5 dB.

The most common use for the Page test is for the detection of a signal onset where, once the signal starts, it does not stop. The Page test has also been suggested for the detection of a temporary change; that is, for detection of finite-duration signals [2], [5], [6]. As described in [2] and [3], the probability of detecting such signals may be approximated through simulation based or analytical methods. Figure 6 contains the probability of detection approximated by the sample cumulative distribution function (CDF) using 2000 samples of the stopping time random variable, the Brownian motion and moment matching methods of [2] and the Poisson mixture method of [3] using 500 samples for  $\bar{T} = 10^3$ , a design SNR of 0 dB, and 0 and 5 dB signal strengths. Similar to the results of [3], the Poisson mixture method provided the best performance as is also indicated by the total squared error between the latter three methods and the sample CDF found in figure 7 as a function of SNR. The decay in the Brownian motion and moment matching approximations may be attributed to the corruption of the auxiliary data by signal presence for lower SNR and to the Page test update being non-Gaussian and a dependent process over time.

The analytical methods of [2] require the unconditional mean and variance of the Page test update. It can be shown that for the complex Gaussian signal with nuisance parameter estimation,

$$E[g] = 2 \left(1 + s - \frac{\tilde{s}}{2}\right) \left(\frac{J}{J-1}\right) - 2 \quad (30)$$

and

$$\text{Var}[g] = \frac{4J^2}{(J-1)(J-2)} \left\{ 1 + 2s + \frac{\left(1 + s - \frac{\tilde{s}}{2}\right)^2}{J-1} \right\}, \quad (31)$$

where, if  $r \sim \text{Gamma}\left(J, \frac{1}{J}\right)$ ,

$$E\left[\frac{1}{r}\right] = \frac{J}{J-1} \quad (32)$$

and

$$E\left[\frac{1}{r^2}\right] = \frac{J^2}{(J-1)(J-2)} \quad (33)$$

have been used.

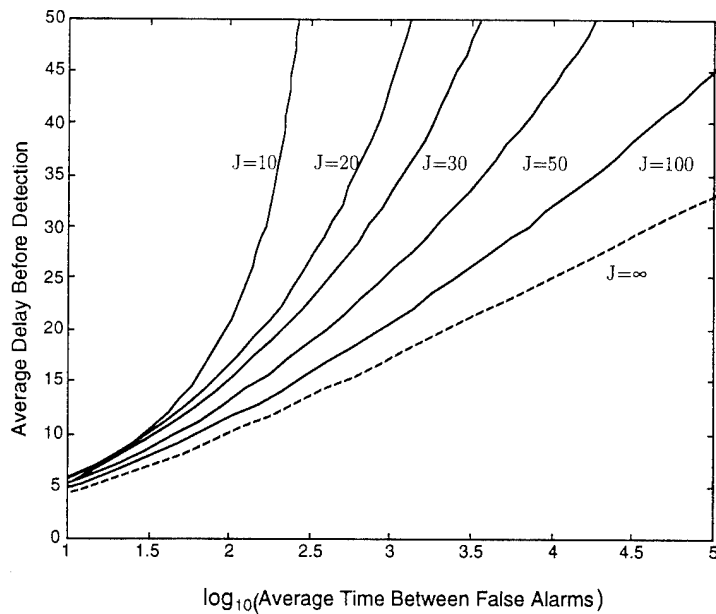


Figure 1. Average Delay Before Detection Vs. Average Time Between False Alarms for 0 dB SNR and Varying Amounts of Auxiliary Data

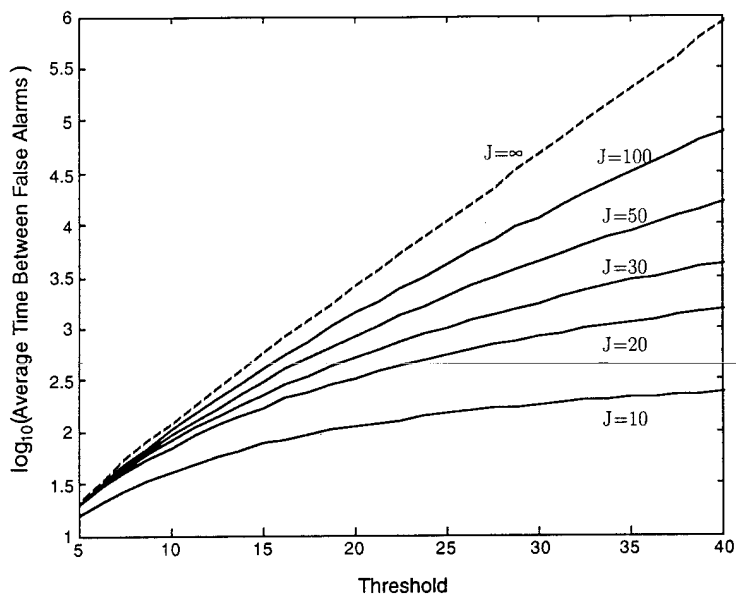


Figure 2. Average Time Between False Alarms Vs. Threshold for Varying Amounts of Auxiliary Data

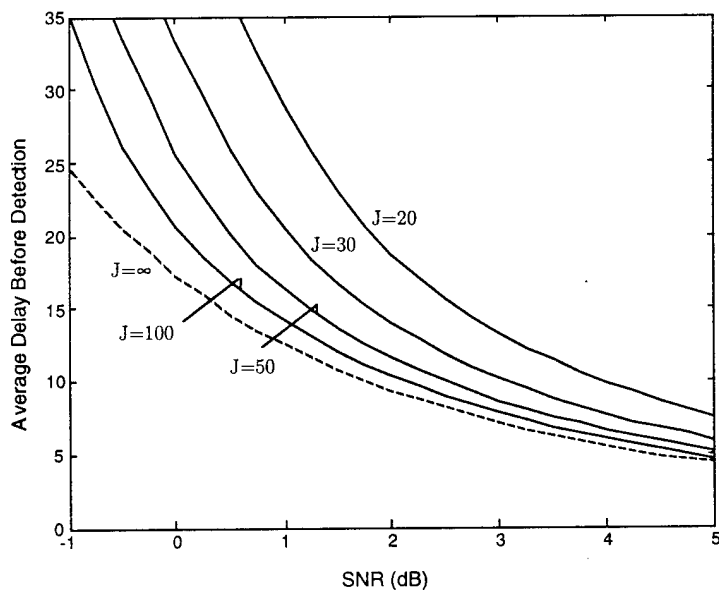


Figure 3. Average Delay Before Detection Vs. SNR for  $\bar{T} = 10^3$  Samples and Varying Amounts of Auxiliary Data

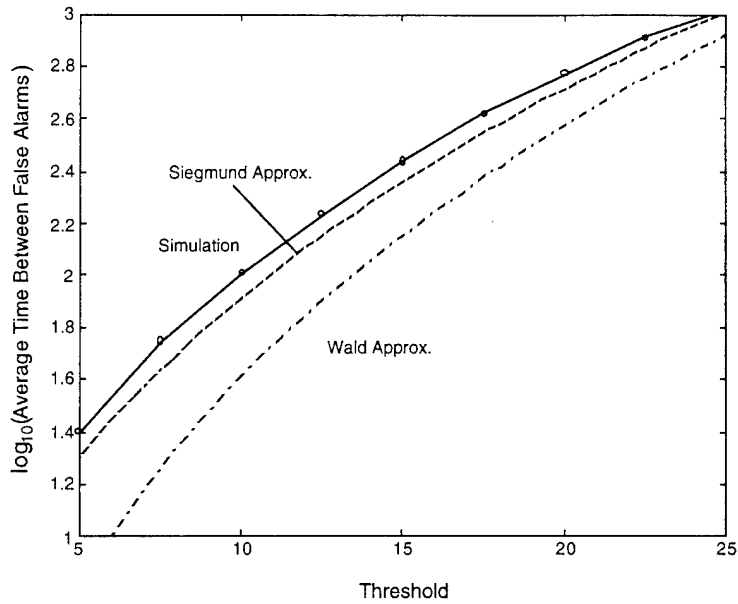


Figure 4. Simulation and Siegmund- and Wald-Based Approximations to Average Time Between False Alarms Vs. Threshold for  $J = 30$

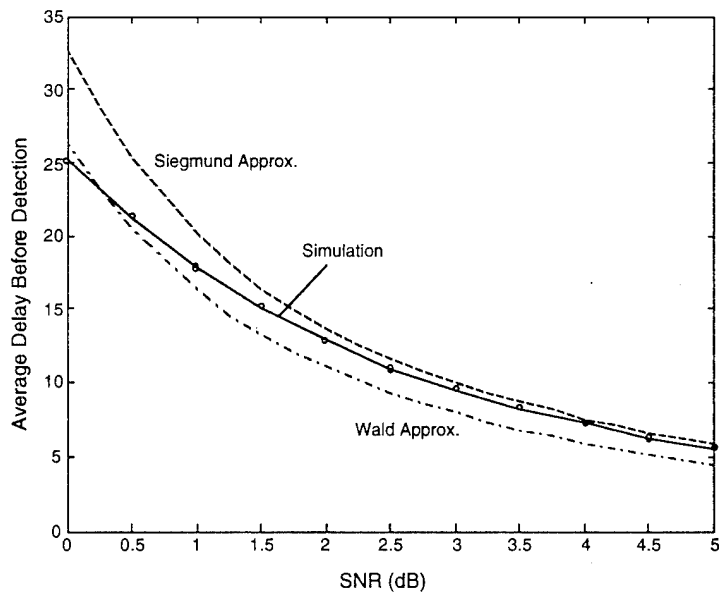


Figure 5. Simulation and Siegmund- and Wald-Based Approximations to Average Delay Before Detection Vs. SNR for  $J = 30$  and  $\bar{T} = 10^3$  Samples

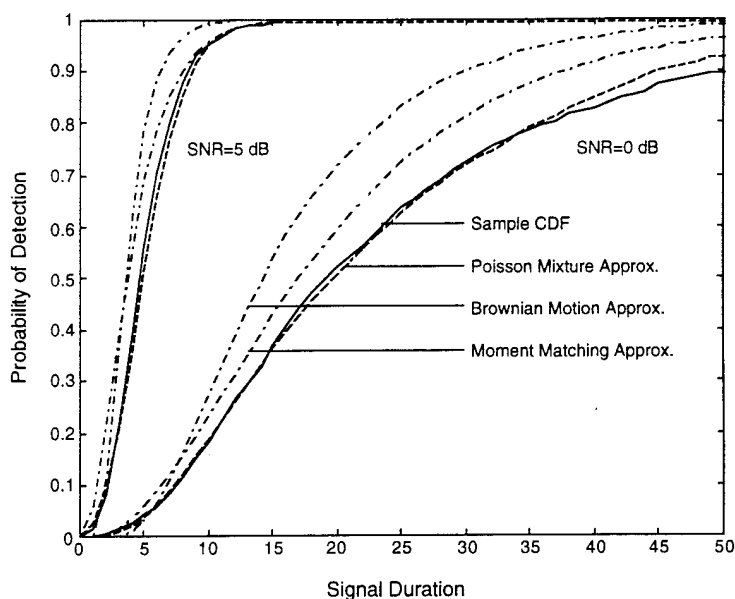


Figure 6. Approximations to the Probability of Detection Vs. Signal Duration for 0 dB and 5 dB SNR,  $J = 30$ , and  $\bar{T} = 10^3$  Samples

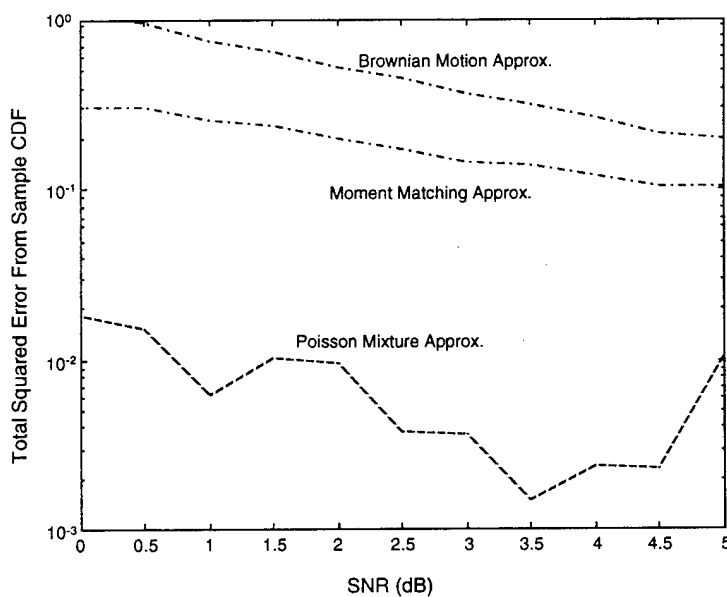


Figure 7. Total Error Between Sample CDF and Probability of Detection Approximations Vs. SNR for  $J = 30$  and  $\bar{T} = 10^3$  Samples

## EXPONENTIAL SIGNAL WITH UNKNOWN NOISE POWER

Exponential data are typically observed as the magnitude squared output of discrete Fourier transforms subject to zero-mean Gaussian random process excitation. When a Gaussian signal is present in the time series data, the mean of the exponential data increases by some unknown amount  $\theta$  from the nominal noise power level  $\lambda$ . In most realistic situations, the noise power  $\lambda$  of the exponential data is unknown.

### STATISTICAL DESCRIPTION

The observed data are assumed to be distributed according to

$$x_i \sim \begin{cases} \text{Exp}(\lambda) & i < q \\ \text{Exp}(\lambda + \theta) & i \geq q \end{cases}, \quad (34)$$

where  $q$  is the unknown starting time of the signal. The notation  $x \sim \text{Exp}(\lambda)$  indicates that the random variable  $x$  has an exponential distribution with mean  $\lambda$  and PDF

$$f(x) = \frac{1}{\lambda} e^{-\frac{x}{\lambda}}, \quad (35)$$

for  $x > 0$ .

### DETECTOR NONLINEARITY

If the nuisance parameter, in this case  $\lambda$ , were known, the detector nonlinearity used in the Page test would be either the LLR or the LO nonlinearity. Here, the LLR and LO nonlinearities result in the same form,

$$\begin{aligned} l(x) &= \log \frac{f_K(x)}{f_H(x)} \\ &= \frac{\theta}{\lambda(\theta + \lambda)} x - \log \left( 1 + \frac{\theta}{\lambda} \right). \end{aligned} \quad (36)$$

Assuming that  $\theta$  is unknown results in scaling equation (36) by  $\frac{\theta+\lambda}{\theta}$  and choosing a design signal strength  $\tilde{\theta}$  for the bias term,

$$\tilde{l}(x) = \frac{x}{\lambda} - \left( \frac{\tilde{\theta} + \lambda}{\tilde{\theta}} \right) \log \left( 1 + \frac{\tilde{\theta}}{\lambda} \right). \quad (37)$$

This is equivalent to using the asymptotically optimal bias [4] on the nonlinearity  $\frac{x}{\lambda}$ . As in the previous section, the Dyson bias results in simpler analysis. The Dyson bias for the above nonlinearity has the form

$$\begin{aligned} \tau &= 1 + \frac{\tilde{\theta}}{2\hat{\lambda}} \\ &= 1 + \frac{\tilde{s}}{2r}, \end{aligned} \quad (38)$$

where  $\tilde{s} = \frac{\tilde{\theta}}{\lambda}$  is a design SNR and

$$r = \frac{\hat{\lambda}}{\lambda} \quad (39)$$

is the normalized estimate of the background noise power.

Thus, the Page test nonlinearity with the Dyson bias and substitution of the nuisance parameter estimate has the form

$$g(x, \hat{\lambda}) = \frac{x}{\hat{\lambda}} - 1 - \frac{\tilde{s}}{2r} \quad (40)$$

$$= \frac{V}{r} - 1 - \frac{\tilde{s}}{2r}, \quad (41)$$

where  $V = \frac{x}{\hat{\lambda}} \sim \text{Exp}(1+s)$  where  $s = \frac{\theta}{\lambda}$  is the actual SNR.

The ASN analysis requires the mean, variance, MGF unity root, and Siegmund correction terms of the detector nonlinearity (40) under hypotheses H and K conditioned on the observed nuisance parameter estimate  $\hat{\lambda}$ . The detector nonlinearity is a scaled and shifted exponential random variable under H and K. A numerical routine for obtaining the MGF unity root is presented in Appendix B. The conditional mean is

$$\begin{aligned} \text{E} \left[ g(x, \hat{\sigma}^2) | \hat{\lambda} \right] &= \frac{\text{E}[V]}{r} - 1 - \frac{\tilde{s}}{2r} \\ &= \frac{1+s}{r} - 1 - \frac{\tilde{s}}{2r} \\ &= \frac{1+s - \frac{\tilde{s}}{2}}{r} - 1, \end{aligned} \quad (42)$$

where here and in the following, hypothesis H is obtained by setting  $s = 0$ . The conditional variance is

$$\begin{aligned} \text{Var} [g(x, \hat{\lambda}) | \hat{\sigma}^2] &= \frac{1}{r^2} \text{Var} [V] \\ &= \frac{(1+s)^2}{r^2}. \end{aligned} \quad (43)$$

The Siegmund correction terms conditioned on  $\hat{\lambda}$  are

$$\rho_{\pm} = (1+s) \frac{\rho_{\pm}^0}{r}, \quad (44)$$

where  $\rho_+^0 = 1$  and  $\rho_-^0 = -\frac{1}{3}$  are as described in [1].

## EXPECTATIONS OVER NUISANCE PARAMETER ESTIMATE

The three expectations over the nuisance parameter estimate required for the Siegmund-based ASN approximation are described in this section for the exponential signal. The nuisance parameter estimate is the MLE of the noise power over the auxiliary data. If the auxiliary data  $(y_1, \dots, y_J)$  are independent and identically distributed according to

$$y_j \sim \text{Exp}(\lambda), \quad (45)$$

the nuisance parameter estimate has the form

$$\hat{\lambda} = \frac{1}{J} \sum_{j=1}^J y_j, \quad (46)$$

which, when scaled by  $\frac{1}{\lambda}$  is easily shown to follow a gamma distribution

$$r = \frac{\hat{\lambda}}{\lambda} \sim \text{Gamma} \left( J, \frac{1}{J} \right). \quad (47)$$

Using the result of equation (18), the first expectation is

$$\begin{aligned} E_1(s) &= \text{E} \left[ \text{E}^{-1} [g | \hat{\lambda}] \right] \\ &= -\text{E} \left[ \frac{r}{r - \left(1 + s - \frac{\bar{s}}{2}\right)} \right] \\ &= -I \left( 1 + s - \frac{\bar{s}}{2}, J, \frac{1}{J} \right). \end{aligned} \quad (48)$$

Using the result of equation (25), the second expectation is

$$\begin{aligned}
 E_2^\pm(s) &= E \left[ \frac{\rho_\pm}{E[g|\hat{\lambda}]} \right] \\
 &= -(1+s)\rho_\pm^0 E \left[ \frac{1}{r - \left(1 + s - \frac{\tilde{s}}{2}\right)} \right] \\
 &= -(1+s)\rho_\pm^0 \frac{[I(1 + s - \frac{\tilde{s}}{2}, J, \frac{1}{J}) - 1]}{\left(1 + s - \frac{\tilde{s}}{2}\right)}. \tag{49}
 \end{aligned}$$

The third expectation has the form

$$\begin{aligned}
 E_3(s) &= E \left[ \frac{t_s \rho_-}{1 - e^{t_s(h + \rho_+ - \rho_-)}} \right] \\
 &= -\frac{1+s}{3} E \left[ \frac{r^{-1} t_s}{1 - e^{t_s(h + r^{-1}(1+s)(\rho_+^0 - \rho_-^0))}} \right] \\
 &= -\frac{1+s}{3} \int_{r=0}^{\infty} \frac{r^{-1} t_s}{1 - e^{t_s(h + \frac{4}{3r}(1+s))}} f(r) dr, \tag{50}
 \end{aligned}$$

where  $t_s$  is the MGF unity root of the Page test update when the scale and bias terms are as found in equation (41). This expectation is easily performed by standard numerical integration with  $t_s$  obtained as a function of the parameters  $(s, \tilde{s}, r)$  using the method described in Appendix B.

## AVERAGE SAMPLE NUMBER AND DETECTION PROBABILITY ANALYSIS

Combining equations (48), (49), and (50) as described in [1] results in the Siegmund-based approximation

$$\begin{aligned}
 A_S(s) &= hE_1(s) + E_2^+(s) - E_2^-(s) + \frac{E_2^-(s)}{E_3(s)} \\
 &= -hI\left(\gamma, J, \frac{1}{J}\right) - \frac{(1+s)}{3\gamma} \left(4 + \frac{1}{E_3(s)}\right) \left[I\left(\gamma, J, \frac{1}{J}\right) - 1\right], \tag{51}
 \end{aligned}$$

where  $\gamma = 1 + s - \frac{\tilde{s}}{2}$ . The average time between false alarms is obtained when  $s = 0$ .

When the nuisance parameter is perfectly estimated (i.e.,  $J \rightarrow \infty$ ),  $r \rightarrow 1$  and the Page test with nuisance parameter estimation results in the standard Page test. In this case, the Siegmund-based approximation to the ASN results is

$$A_S^\infty(s) = \frac{1 + t_s h_s - e^{t_s h_s}}{t_s \left(s - \frac{\tilde{s}}{2}\right)}, \tag{52}$$

where

$$\begin{aligned} h_s &= h + \rho_+ - \rho_- \\ &= h + \frac{4}{3}(1 + s), \end{aligned} \quad (53)$$

and  $t_s$  is, as before, the MGF unity root where  $r = 1$  in the scale and bias terms of equation (41).

The above Siegmund-based approximations to the average time between false alarms ( $s = 0$ ) and the average delay before detection ( $s > 0$ ) are used to evaluate the performance of the Page test with nuisance parameter estimation for the exponential signal. Figure 8 contains the Page test OC curve for  $s = 0$  dB, a design SNR  $\tilde{s} = 0$  dB, and for auxiliary data amounts  $J = 10, 20, 30, 50, 100$ , and  $\infty$  (perfect estimation of the nuisance parameter). Curves of the average time between false alarms as a function of the threshold for the above situation are found in figure 9. The average delay before detection as a function of SNR is found in figure 10 where the design SNR and average time between false alarms are held constant at  $\tilde{s} = 0$  dB and  $\bar{T} = 10^3$  respectively. Note that in this situation there is a MDL that increases as  $J$  decreases (note that the MDL for  $J = \infty$  is approximately  $-3$  dB).

Simulations are performed to validate the approximations to  $\bar{T}$  and  $\bar{D}$  and to evaluate the performance of existing methods for approximating the probability of detecting a finite-duration signal using the Page test with nuisance parameter estimation. Figures 11 and 12 contain the Siegmund- and Wald-based approximations to  $\bar{T}$  and  $\bar{D}$  along with that estimated from simulation. In all cases, the design SNR is 0 dB and  $J = 30$  samples of auxiliary data are used to estimate the nuisance parameter with a buffer of equivalent length. The thresholds for the results shown in figure 12 are set according to  $\bar{T} = 10^3$ . The discrepancy between the Siegmund-based approximations and the simulations at lower SNR is the result of an inadequate buffer size. In this situation, the nuisance parameter estimate is often corrupted by data containing signal, particularly for SNRs below 1 dB. Unfortunately, the solution to this problem suggested in [1], requiring estimation of the nuisance parameter under the signal-present hypothesis, is not suitable for the exponential signal. Thus, the buffer zone separating the auxiliary data from the current test sample must be carefully designed.

Figure 13 contains the probability of detection approximated by the sample CDF using

2000 samples of the stopping time random variable, the Brownian motion and moment matching methods of [2] and the Poisson mixture method of [3] using 500 samples for  $\bar{T} = 10^3$ , a design SNR of 0 dB, and 0 and 5 dB signal strengths. Similar to the results of [3], the Poisson mixture method provided the best performance as is also indicated by the total squared error between the latter three methods and the sample CDF found in figure 14 as a function of SNR.

The analytical methods of [2] require the unconditional mean and variance of the Page test update. It can be shown that for the exponential signal with nuisance parameter estimation,

$$E[g] = \left(1 + s - \frac{\tilde{s}}{2}\right) \left(\frac{J}{J-1}\right) - 1 \quad (54)$$

and

$$\text{Var}[g] = \frac{J^2}{(J-1)(J-2)} \left\{ (1+s)^2 + \frac{\left(1 + s - \frac{\tilde{s}}{2}\right)^2}{J-1} \right\}, \quad (55)$$

where, equations (32) and (33) have been used.

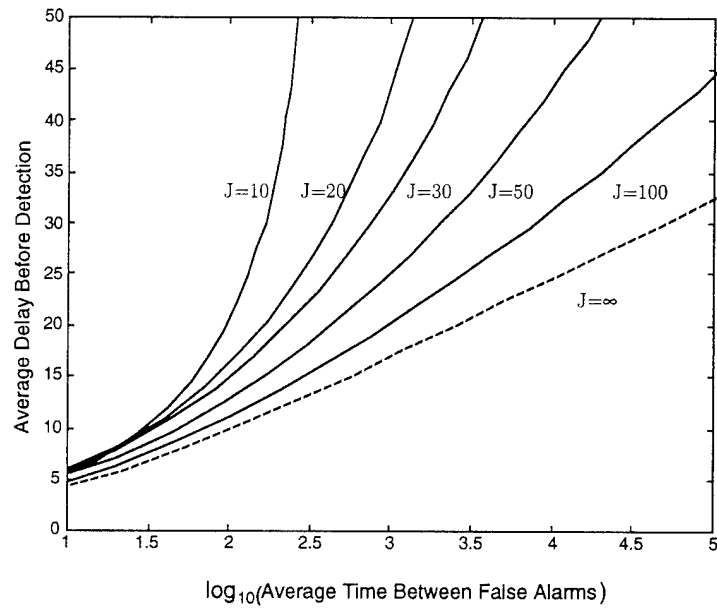


Figure 8. Average Delay Before Detection Vs. Average Time Between False Alarms for 0 dB SNR, and Varying Amounts of Auxiliary Data

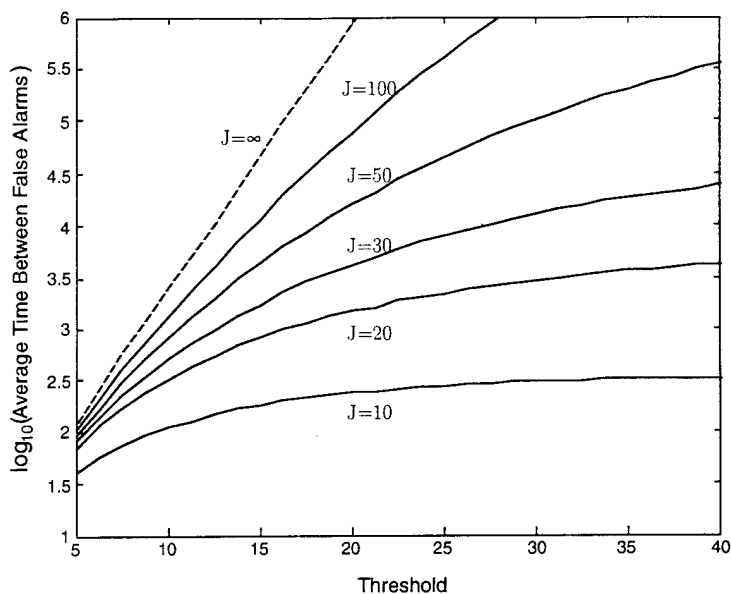


Figure 9. Average Time Between False Alarms Vs. Threshold for Varying Amounts of Auxiliary Data

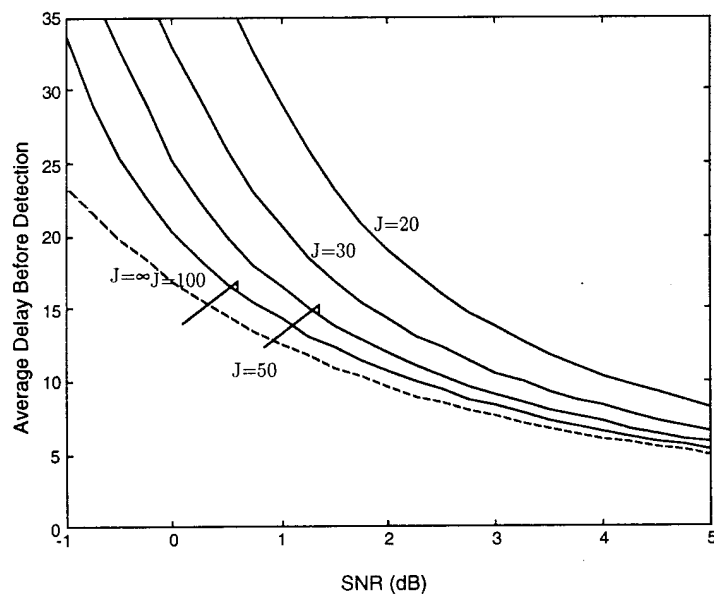


Figure 10. Average Delay Before Detection Vs. SNR for  $\bar{T} = 10^3$  Samples and Varying Amounts of Auxiliary Data

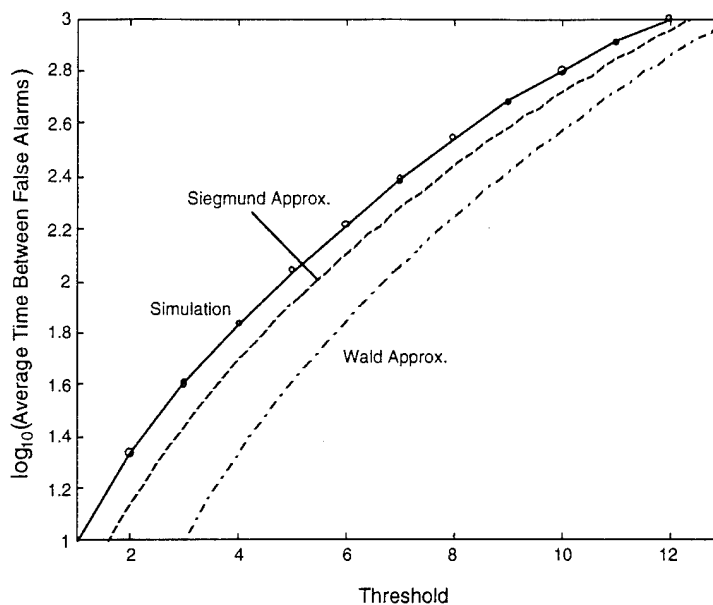


Figure 11. Simulation and Siegmund- and Wald-Based Approximations to Average Time Between False Alarms Vs. Threshold for  $J = 30$

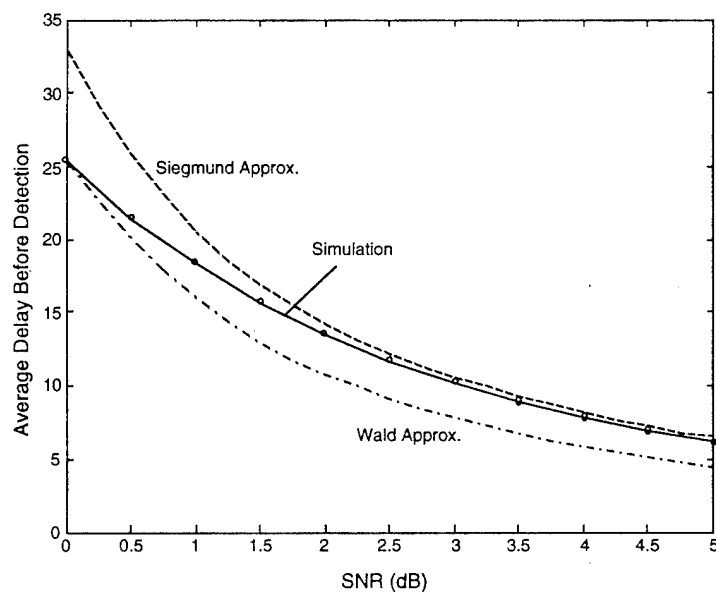


Figure 12. Simulation and Siegmund- and Wald-Based Approximations to Average Delay Before Detection Vs. SNR for  $J = 30$  and  $\bar{T} = 10^3$  Samples

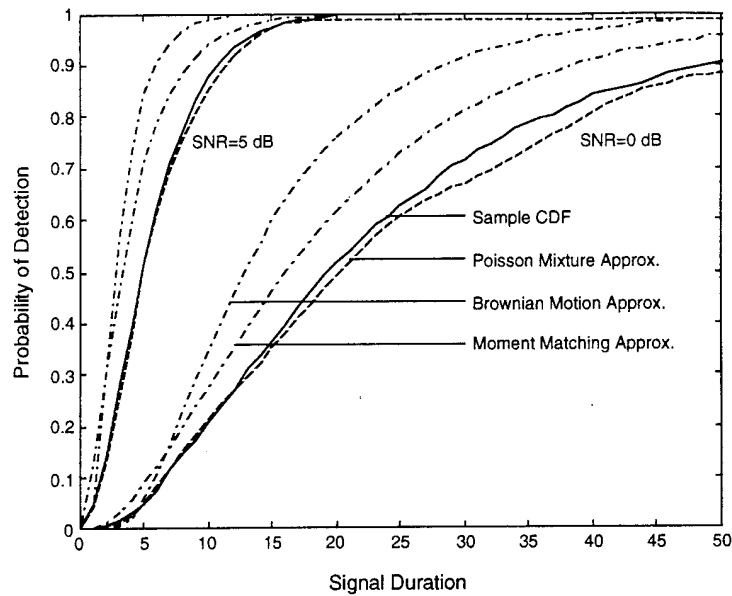


Figure 13. Approximations to the Probability of Detection Vs. Signal Duration for 0 dB and 5 dB SNR,  $J = 30$ , and  $\bar{T} = 10^3$  Samples

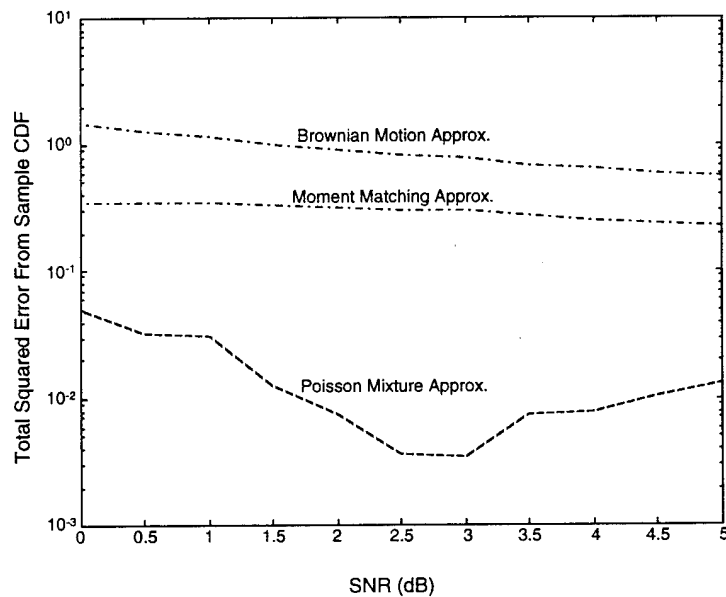


Figure 14. Total Error Between Sample CDF and Probability of Detection Approximations Vs. SNR for  $J = 30$  and  $\bar{T} = 10^3$  Samples

## MULTIVARIATE COMPLEX GAUSSIAN DETERMINISTIC SIGNAL WITH UNKNOWN INTERFERENCE COVARIANCE MATRIX

The multivariate complex Gaussian deterministic signal arises as an extension of the complex Gaussian shift in mean signal to multiple sensor observations. The unknown variance extends to an unknown covariance matrix. The multivariate deterministic signal model represents a sinusoidal signal with unknown phase received by an array of sensors and results in an unknown complex amplitude scaling a known direction or steering vector as the mean of the vector observation.

### STATISTICAL DESCRIPTION

The observed data are assumed to be distributed according to

$$\mathbf{x}_i \sim \begin{cases} \mathcal{CN}_N(0, \Sigma) & i < q \\ \mathcal{CN}_N(\theta \mathbf{d}, \Sigma) & i \geq q \end{cases}, \quad (56)$$

where  $\Sigma$  is the unknown interference covariance matrix of the observed data,  $\theta$  is the unknown complex amplitude of the signal,  $\mathbf{d}$  is a known array steering vector, and  $q$  is the unknown starting time of the signal. The notation  $\mathbf{x} \sim \mathcal{CN}_N(\mu, \Sigma)$  indicates that the length  $N$  random vector  $\mathbf{x}$  has a multivariate complex Gaussian distribution with mean  $\mu$ , covariance matrix  $\Sigma$ , and PDF

$$f(\mathbf{x}) = \frac{1}{\pi^N |\Sigma|} e^{-(\mathbf{x}-\mu)^H \Sigma^{-1} (\mathbf{x}-\mu)}, \quad (57)$$

for  $\mathbf{x} \in \mathcal{C}^N$ , where the superscript  $H$  indicates the complex conjugate and transpose operation. It is assumed that the steering vector  $\mathbf{d}$  has unit length,  $\mathbf{d}^H \mathbf{d} = 1$ .

### DETECTOR NONLINEARITY

If the nuisance parameter  $\Sigma$  were known, the detector nonlinearity used in the Page test would be either a LO or GLR nonlinearity. As with the univariate case, direct application

of the LO nonlinearity is not straightforward. However, the GLR nonlinearity may be easily derived by describing the LLR as

$$\begin{aligned}
 l(\mathbf{x}) &= \log \frac{f_K(\mathbf{x})}{f_H(\mathbf{x})} \\
 &= \mathbf{x}^H \boldsymbol{\Sigma}^{-1} \mathbf{x} - (\mathbf{x} - \theta \mathbf{d})^H \boldsymbol{\Sigma}^{-1} (\mathbf{x} - \theta \mathbf{d}) \\
 &= \frac{|\mathbf{d}^H \boldsymbol{\Sigma}^{-1} \mathbf{x}|^2}{\mathbf{d}^H \boldsymbol{\Sigma}^{-1} \mathbf{d}} - \mathbf{d}^H \boldsymbol{\Sigma}^{-1} \mathbf{d} \left| \theta - \frac{\mathbf{d}^H \boldsymbol{\Sigma}^{-1} \mathbf{x}}{\mathbf{d}^H \boldsymbol{\Sigma}^{-1} \mathbf{d}} \right|^2.
 \end{aligned} \tag{58}$$

The GLR statistic is the maximum of the LLR over all possible values of the unknown complex signal amplitude  $\theta$ . Maximizing equation (58) clearly requires choosing  $\hat{\theta} = \frac{\mathbf{d}^H \boldsymbol{\Sigma}^{-1} \mathbf{x}}{\mathbf{d}^H \boldsymbol{\Sigma}^{-1} \mathbf{d}}$  which leads to the GLR statistic

$$V = 2 \frac{|\mathbf{d}^H \boldsymbol{\Sigma}^{-1} \mathbf{x}|^2}{\mathbf{d}^H \boldsymbol{\Sigma}^{-1} \mathbf{d}}. \tag{59}$$

Using Theorem 1 of [7] it is straightforward to show that if  $\mathbf{x} \sim \mathcal{CN}_N(\mu, \boldsymbol{\Sigma})$  then

$$2 \frac{|\mathbf{w}^H \mathbf{x}|^2}{\mathbf{w}^H \boldsymbol{\Sigma} \mathbf{w}} \sim \chi_2^2(\delta), \tag{60}$$

where the noncentrality parameter is

$$\delta = 2 \frac{|\mathbf{w}^H \mu|^2}{\mathbf{w}^H \boldsymbol{\Sigma} \mathbf{w}}. \tag{61}$$

Applying this to equation (59) with  $\mathbf{w} = \boldsymbol{\Sigma}^{-1} \mathbf{d}$ , it is seen that

$$V \sim \chi_2^2(\delta), \tag{62}$$

where

$$\begin{aligned}
 \delta &= 2 |\theta|^2 \mathbf{d}^H \boldsymbol{\Sigma}^{-1} \mathbf{d} \\
 &= 2s.
 \end{aligned} \tag{63}$$

Thus, the bias required for application of this test statistic to the Page test may be chosen in the same manner as the univariate case (equation (6)).

Upon substitution of the nuisance parameter estimate,  $\hat{\boldsymbol{\Sigma}}$ , the Page test nonlinearity has the form

$$g(x, \hat{\boldsymbol{\Sigma}}) = 2 \frac{|\mathbf{d}^H \hat{\boldsymbol{\Sigma}}^{-1} \mathbf{x}|^2}{\mathbf{d}^H \hat{\boldsymbol{\Sigma}}^{-1} \mathbf{d}} - 2 - \bar{a} \mathbf{d}^H \hat{\boldsymbol{\Sigma}}^{-1} \mathbf{d} \tag{64}$$

$$\begin{aligned}
&= 2 \frac{|\hat{\mathbf{w}}^H \mathbf{x}|^2}{\hat{\mathbf{w}}^H \hat{\Sigma} \hat{\mathbf{w}}} \left( \frac{\hat{\mathbf{w}}^H \Sigma \hat{\mathbf{w}}}{\mathbf{d}^H \hat{\Sigma}^{-1} \mathbf{d}} \right) - 2 - \tilde{s} \frac{\mathbf{d}^H \hat{\Sigma}^{-1} \mathbf{d}}{\mathbf{d}^H \Sigma^{-1} \mathbf{d}} \\
&= V \left( \frac{\mathbf{d}^H \hat{\Sigma}^{-1} \Sigma \hat{\Sigma}^{-1} \mathbf{d}}{\mathbf{d}^H \hat{\Sigma}^{-1} \mathbf{d}} \right) - 2 - \tilde{s} \frac{\mathbf{d}^H \hat{\Sigma}^{-1} \mathbf{d}}{\mathbf{d}^H \Sigma^{-1} \mathbf{d}}, \tag{65}
\end{aligned}$$

where  $\tilde{\theta} = |\tilde{\theta}|^2$  is a design signal power,  $\tilde{s} = \tilde{\theta} \mathbf{d}^H \Sigma^{-1} \mathbf{d}$  is a design signal-to-interference power ratio (SIR), and  $\hat{\mathbf{w}} = \hat{\Sigma}^{-1} \mathbf{d}$ . By applying equations (60) and (61), it is seen that  $V$  is noncentral chi-squared distributed,

$$V = 2 \frac{|\hat{\mathbf{w}}^H \mathbf{x}|^2}{\hat{\mathbf{w}}^H \Sigma \hat{\mathbf{w}}} \sim \chi_2^2(\delta), \tag{66}$$

with noncentrality parameter

$$\begin{aligned}
\delta &= 2 \frac{|\hat{\mathbf{w}}^H(\theta \mathbf{d})|^2}{\hat{\mathbf{w}}^H \Sigma \hat{\mathbf{w}}} \\
&= 2 |\theta|^2 \frac{(\mathbf{d}^H \hat{\Sigma}^{-1} \mathbf{d})^2}{\mathbf{d}^H \hat{\Sigma}^{-1} \Sigma \hat{\Sigma}^{-1} \mathbf{d}}. \tag{67}
\end{aligned}$$

Defining

$$r = \frac{\mathbf{d}^H \Sigma^{-1} \mathbf{d}}{\mathbf{d}^H \hat{\Sigma}^{-1} \mathbf{d}} \tag{68}$$

and

$$p = \frac{(\mathbf{d}^H \hat{\Sigma}^{-1} \mathbf{d})^2}{(\mathbf{d}^H \hat{\Sigma}^{-1} \Sigma \hat{\Sigma}^{-1} \mathbf{d}) (\mathbf{d}^H \Sigma^{-1} \mathbf{d})}, \tag{69}$$

the Page test nonlinearity may be written as

$$g(x, \hat{\Sigma}) = \frac{V}{pr} - 2 - \frac{\tilde{s}}{r} \tag{70}$$

and the noncentrality parameter of  $V$  as  $\delta = 2sp$ .

The ASN analysis requires the mean, MGF unity root, and Siegmund correction terms of the detector nonlinearity (70) under hypotheses H and K conditioned on the observed nuisance parameter estimate  $\hat{\Sigma}$ . As the detector nonlinearity is a scaled and shifted noncentral chi-squared random variable under H and K, the numerical routine presented in Appendix A

may be used for obtaining the MGF unity root. The conditional mean is

$$\begin{aligned} \mathbb{E} \left[ g(x, \hat{\Sigma}) \mid \hat{\Sigma} \right] &= \frac{\mathbb{E}[V]}{pr} - 2 - \frac{\tilde{s}}{r} \\ &= \frac{2 + 2sp}{pr} - 2 - \frac{\tilde{s}}{r} \\ &= \frac{2}{pr} \left[ 1 + p \left( s - \frac{\tilde{s}}{2} \right) \right] - 2, \end{aligned} \quad (71)$$

where here and in the following, hypothesis H is obtained by setting  $\delta = s = 0$ . The Siegmund correction terms conditioned on  $\hat{\Sigma}$  are

$$\rho_{\pm}^{\delta} = \frac{\rho_{\pm}^{\delta}}{pr}, \quad (72)$$

where  $\rho_{\pm}^{\delta}$  are as previously described, except here  $\delta = 2sp$ .

## EXPECTATIONS OVER NUISANCE PARAMETER ESTIMATE

The three expectations over the nuisance parameter estimate required for the Siegmund-based ASN approximation are described in this section for the multivariate complex Gaussian data with a deterministic array signal. The nuisance parameter estimate is the MLE of the interference covariance matrix over the auxiliary data. If the auxiliary data  $(\mathbf{y}_1, \dots, \mathbf{y}_J)$  are independent and identically distributed according to

$$\mathbf{y}_j \sim \mathcal{CN}_N(\mathbf{0}, \Sigma), \quad (73)$$

the nuisance parameter estimate has the form

$$\hat{\Sigma} = \frac{1}{J} \sum_{j=1}^J \mathbf{y}_j \mathbf{y}_j^H, \quad (74)$$

which is distributed according to the scale of a complex Wishart distributed matrix,

$$J\hat{\Sigma} \sim \mathcal{CW}_N(J, \Sigma), \quad (75)$$

where the notation  $\mathbf{A} \sim \mathcal{CW}_N(J, \Sigma)$  indicates that the  $N$ -by- $N$  random matrix  $\mathbf{A}$  has a complex Wishart distribution with  $J$  degrees of freedom and  $\Sigma$  for a scale matrix. Utilizing this and the results stated in Appendix A of [8] it is seen that  $r$  of equation (68) is gamma distributed

$$r \sim \text{Gamma} \left( J - N + 1, \frac{1}{J} \right) \quad (76)$$

with PDF

$$f(r) = \frac{J^{J-N+1} r^{J-N} e^{-Jr}}{\Gamma(J-N+1)} \quad (77)$$

for  $r > 0$ , and that  $p$  of equation (69) is beta distributed

$$p \sim \text{Beta}(J-N+2, N-1), \quad (78)$$

with PDF

$$f(p) = \frac{\Gamma(J+1) p^{J-N+1} (1-p)^{N-2}}{\Gamma(J-N+2) \Gamma(N-1)}, \quad (79)$$

for  $0 < p < 1$ .

Using the result of equation (18), the first expectation is

$$\begin{aligned} E_1(s) &= E_{\hat{\Sigma}} \left[ E^{-1} [g|\hat{\Sigma}] \right] \\ &= -\frac{1}{2} E_{pr} \left[ \frac{r}{r - \left( \frac{1}{p} + s - \frac{\tilde{s}}{2} \right)} \right] \\ &= -\frac{1}{2} E_p \left[ I \left( \frac{1}{p} + s - \frac{\tilde{s}}{2}, J-N+1, \frac{1}{J} \right) \right], \end{aligned} \quad (80)$$

where subscripts on expectations indicate the random variable over which the expectation is performed.

Using the result of equation (25), the second expectation is

$$\begin{aligned} E_2^\pm(s) &= E_{\hat{\Sigma}} \left[ \frac{\rho_\pm}{E[g|\hat{\Sigma}]} \right] \\ &= -E_p \left[ \frac{\rho_\pm^\delta}{2p} E_r \left[ \frac{1}{r - \left( \frac{1}{p} + s - \frac{\tilde{s}}{2} \right)} \right] \right] \\ &= -E_p \left[ \frac{\rho_\pm^\delta \left\{ I \left( \frac{1}{p} + s - \frac{\tilde{s}}{2}, J-N+1, \frac{1}{J} \right) - 1 \right\}}{2 + 2p \left( s - \frac{\tilde{s}}{2} \right)} \right]. \end{aligned} \quad (81)$$

The third expectation has the form

$$\begin{aligned} E_3(s) &= E \left[ \frac{t_s \rho_-}{1 - e^{t_s(h+\rho_+-\rho_-)}} \right] \\ &= E_{rp} \left[ \frac{\rho_-^\delta (rp)^{-1} t_s}{1 - e^{t_s(h+(rp)^{-1}(\rho_+^\delta - \rho_-^\delta))}} \right] \\ &= \int_{p=0}^1 \int_{r=0}^\infty \frac{\rho_-^\delta (rp)^{-1} t_s f(r) f(p)}{1 - \exp \left\{ t_s \left( h + \frac{\rho_+^\delta - \rho_-^\delta}{rp} \right) \right\}} dr dp, \end{aligned} \quad (82)$$

where  $t_s$  is the MGF unity root of the Page test update when  $\delta = 2sp$  is the noncentrality parameter and the scale and bias terms are as found in equation (70). This expectation is easily performed by standard numerical integration with  $t_s$  obtained as a function of the parameters  $(s, \bar{s}, r, p)$  using the method described in Appendix A.

Note that when  $N = 1$ ,  $p$  becomes a degenerate random variable with value one ( $p \rightarrow 1$ ) and all of the results of this section simplify to those of the univariate case previously described.

### AVERAGE SAMPLE NUMBER ANALYSIS

Combining equations (80), (81), and (82) as described in [1] results in the Siegmund-based approximation

$$\begin{aligned} A_S(s) &= hE_1(s) + E_2^+(s) - E_2^-(s) + \frac{E_2^-(s)}{E_3(s)} \\ &= \frac{-h}{2} E_p \left[ I \left( \gamma, J - N + 1, \frac{1}{J} \right) \right] \\ &\quad - E_p \left[ \left\{ \rho_+^\delta - \rho_-^\delta + \frac{\rho_-^\delta}{E_3(s)} \right\} \left\{ \frac{I \left( \gamma, J - N + 1, \frac{1}{J} \right) - 1}{2p\gamma} \right\} \right], \end{aligned} \quad (83)$$

where  $\gamma = \frac{1}{p} + s - \frac{\bar{s}}{2}$ . The average time between false alarms is obtained when  $\delta = s = 0$ .

When the nuisance parameter is perfectly estimated (i.e.,  $J \rightarrow \infty$ ),  $r \rightarrow 1$  and  $p \rightarrow 1$  and the Page test with nuisance parameter estimation results in the standard Page test. In this case, the Siegmund-based approximation to the ASN is identical to that of equation (29) with  $s = |\theta|^2 \mathbf{d}^H \boldsymbol{\Sigma}^{-1} \mathbf{d}$ .

The above Siegmund-based approximations to the average time between false alarms ( $s = 0$ ) and the average delay before detection ( $s > 0$ ) are used to evaluate the performance of the Page test with nuisance parameter estimation for the complex Gaussian shift in mean signal. In all cases, the adaptive dimension is  $N = 5$  and the design SNR is 0 dB. First, the approximations are compared to simulation in figures 15 and 16 for  $J = 30$  as a function of threshold. The Siegmund-based approximations for varying amounts of auxiliary data ( $J = 25, 30, 40, 50, 60, 75, 100$ , and  $\infty$ ) as a function of threshold are found in figures 17 and 18.

Figure 18 contains the Page test OC curve for  $s = 0$  dB and a design SNR  $\tilde{s} = 0$  dB for auxiliary data amounts (perfect estimation of the nuisance parameter). Curves of the average time between false alarms as a function of the threshold for above situation are found in figure 17. Curves of the average delay before detection as a function of threshold are found in figure 18.

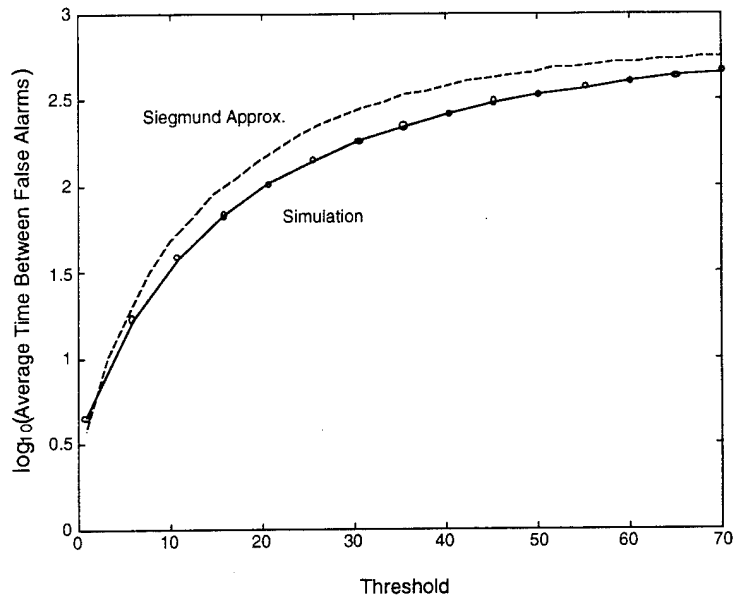


Figure 15. Simulation and Siegmund-Based Approximation to Average Time Between False Alarms Vs. Threshold for  $N = 5$  and  $J = 30$

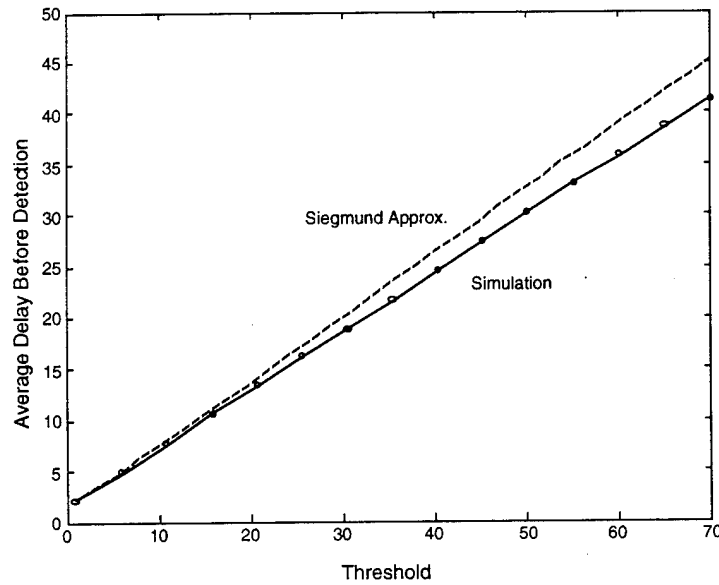


Figure 16. Simulation and Siegmund-Based Approximation to Average Delay Before Detection Vs. Threshold for  $N = 5$ ,  $J = 30$ , and 0 dB SNR

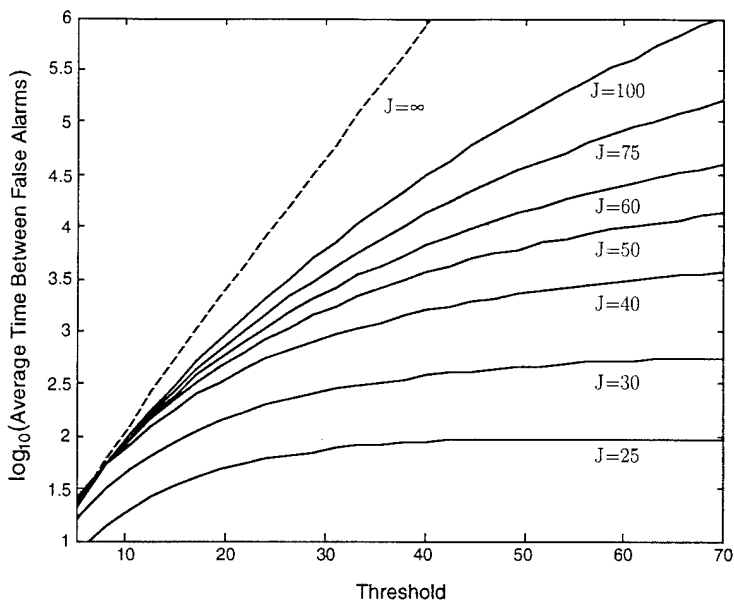


Figure 17. Average Time Between False Alarms Vs. Threshold for 0 dB SNR,  $N = 5$ , and Varying Amounts of Auxiliary Data

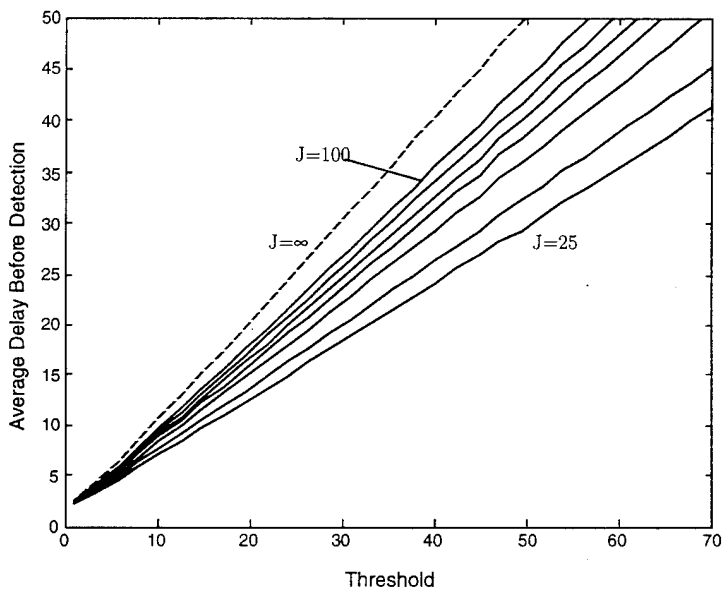


Figure 18. Average Delay Before Detection Vs. Threshold for 0 dB SNR,  $N = 5$ , and Varying Amounts of Auxiliary Data

## NONPARAMETRIC CHANGE DETECTION

The nuisance parameter estimation concept of [1] may be extended to the nonparametric detection problem. In this situation, the PDF of the observed data is unknown under both the signal-absent and signal-present hypotheses. The signal-present hypothesis is solely distinguished from the signal-absent hypothesis by general functional relationships between the signal-absent CDF,  $F(x)$ , and the signal-present CDF,  $G(x)$ . Common relationships include a change in location parameter,  $G(x) = F(x - \delta)$ , change in scale parameter,  $G(x) = F\left(\frac{x}{\delta}\right)$  or relationships such as Lehmann alternatives  $G(x) = [F(x)]^\delta$  where  $\delta > 0$  and not equal to one. Thus, the *nuisance parameter* is the actual PDF under the signal-absent hypothesis.

Application of the technique described in [1] to nonparametric change detection first requires assuming that the change (signal) has not occurred up to the current time (referenced by the index  $i$ ). A sequential test between the null hypothesis ( $G(x) = F(x)$ ) and one of the above alternatives is then performed where data distributed under  $F$  are obtained from time samples  $i - K, i - K - 1, \dots, i - K - L + 1$  where  $K$  represents a buffer ensuring that these auxiliary data are signal-free and  $L$  is the maximum number of available auxiliary data samples, governed by the stationarity of the noise sequence. Data distributed under  $G$  (which is either  $F$  under the signal-absent hypothesis or one of the above alternatives in the signal-present hypothesis) are then obtained from time samples  $i + 1, i + 2, \dots$ , until a decision between signal-absence and signal-presence is made, say at time index  $i + M$ . If a signal-present decision is made, the test is stopped with stopping time  $N = i + M$ . If a signal-absent decision is made, then the procedure is repeated after setting  $i = i + M$ . Thus, the test has the same framework as the Page test with nuisance parameter estimation, and results in the same ASN of equation (39) in [1]. Evaluation of this requires the ASNs and operating characteristic of the individual nonparametric sequential tests used to implement this nonparametric change point detector, which, depending on the test, may not be straightforward to determine. Important in this evaluation is that the ASNs and operating characteristic are determined accounting for the randomness of the auxiliary data.

In [1], and in the previous sections of this report, this is done by conditioning on a nuisance parameter estimate followed by an expectation removing the conditioning. This approach may or may not apply to any given nonparametric sequential test. Govindarajulu [9] and Sen in [10] describe several sequential nonparametric tests, including two-sample tests such as that of Savage and Sethuraman.

It may be possible to modify this type of nonparametric change detection problem to allow a parameterized noise only distribution with unknown nuisance parameters and sequential testing for some sort of generic change indicating signal-presence.

## CONCLUSIONS

The Page test with nuisance parameter estimation [1] was applied to the detection of the following signal types: (i) complex Gaussian distributed data with a shift in mean signal and unknown variance, (ii) exponentially distributed data with an unknown noise power, and (iii) multivariate complex Gaussian distributed data with a deterministic array signal and an unknown interference covariance matrix.

For each signal type, a detector nonlinearity was developed from either LO or GLR principles and use of the Dyson bias [4], and the corresponding Siegmund-based approximations to the ASN derived. The Siegmund- and Wald-based approximations were compared to simulation for the average time between false alarms and average delay before detection where it was observed that the Siegmund-based approximations are more accurate. Corruption of the nuisance parameter estimate by auxiliary data containing both signal and noise components was observed for weaker signal strengths. This may be avoided by proper design of the buffer zone between the auxiliary data and the current data sample. For instance, the buffer size may be chosen so that minimal corruption occurs for the smallest signal level desired to be detected. Operating characteristic curves for each of the signal types were generated describing the performance of the detectors as a function of threshold and SNR.

The probability of detecting a finite duration signal was approximated by the Brownian motion and moment matching approximations of [2] and estimated by the Poisson mixture method of [3] where it was observed that the Poisson mixture method provided the minimum total estimation error. This is an expected result as the approximation methods of [2] are based on the assumption of a Page test update sequence that is independent in time and, in the Brownian motion case, has Gaussian update statistics. Use of the nuisance parameter estimate in the Page test update introduces correlation into the update sequence. The Poisson mixture method simply models the PDF of the stopping time by a mixture of Poisson random variables. It should be noted that, as indicated by the results of [11], this approximation may be improved by including a single geometric component in the mixture

to correctly model the tail probability.

As with most GLR techniques, the only optimality associated with the nonlinearity choice for the above signal types is asymptotic as the amount of auxiliary data becomes infinite. Thus, it is feasible that the performance of these signal detectors may be improved by a modification of the nonlinearity. For instance, the asymptotically optimal bias of [4] may be used rather than the Dyson bias. However, as previously mentioned, this results in a more difficult theoretical analysis of the detector performance. Other modifications may include the use of a design SNR in the detector implementation rather than a design signal strength or inclusion of the statistics of the nuisance parameter estimate into the nonlinearity formulation.

Signal-onset detection where signal-presence is distinguished from signal-absence solely by a functional relationship between the CDFs of the data was discussed within the framework of the Page test with nuisance parameter estimation.

## REFERENCES

- [1] D. A. Abraham, "A Page Test With Nuisance Parameter Estimation," Technical Report 10,829, Naval Undersea Warfare Center Detachment, New London, CT, 1 March 1995.
- [2] C. Han, P. K. Willett, and D. A. Abraham, "Some Bounds and Approximations to the Probability of Detection of a Transient Signal," Technical Report 94-4, University of Connecticut, Storrs, CT, October 1994.
- [3] D. A. Abraham, "Approximation of the Page Test Probability of Detection by the Cumulative Distribution of a Mixture of Poisson Random Variables," Technical Report 10,793, Naval Undersea Warfare Center Detachment, New London, CT, 1 December 1994.
- [4] D. A. Abraham, "Asymptotically Optimal Bias for a General Non-linearity in Page's Test," *IEEE Transactions on Aerospace and Electronic Systems*, 1995 (To be published, July 1995).
- [5] B. Broder, "Quickest Detection Procedures and Transient Signal Detection," Ph.D Dissertation, Princeton University, Princeton, NJ, 1990.
- [6] D. A. Abraham, "Sequential vs. Sliding Fixed Block Detection of Finite Unknown Duration Signals," in *Proceedings of The Technical Cooperation Program, Twenty-Third Annual International Meeting*, Auckland, New Zealand, November 1994.
- [7] D. A. Abraham, "Statistical Theorems Involving the Complex Multivariate Gaussian and Wishart Densities," Technical Memorandum 931133, Naval Undersea Warfare Center Detachment, New London, CT, 13 September 1993.
- [8] D. A. Abraham, "A Maximum Likelihood Based Adaptive Detector," Technical Memorandum 941021, Naval Undersea Warfare Center Detachment, New London, CT, April 1994.
- [9] Z. Govindarajulu, *The Sequential Statistical Analysis of Hypothesis Testing, Point and Interval Estimation, and Decision, Theory*, American Sciences Press, Inc., 1987.
- [10] B. K. Ghosh and P. K. Sen, eds., *Handbook of Sequential Analysis*, Marcel Dekker, Inc., 1991.
- [11] C. Han, P. K. Willett, and D. A. Abraham, "False Alarm Time Distributions in Page's Test," in *Proceedings of 1995 Conference on Information Sciences and Systems*, March 1995.

**APPENDIX A: MGF UNITY ROOT FOR A NONCENTRAL  
CHI-SQUARED RANDOM VARIABLE**

Suppose that a Page test update has the form

$$g(Y) = aY - b, \quad (\text{A-1})$$

where  $a > 0$  and the data  $Y$  has a noncentral chi-squared distribution with  $n$  degrees of freedom and a noncentrality parameter  $\delta$ .

The nonzero unity root of the moment generating function (MGF) of  $g(Y)$  is the value of  $t$  satisfying

$$E[e^{tg(Y)}] = M(t) = 1. \quad (\text{A-2})$$

The MGF of  $g$  may be obtained from the MGF of a noncentral chi-squared random variable by

$$\begin{aligned} M(t) &= E[e^{t(aY-b)}] \\ &= e^{-bt} E[e^{(at)Y}] \\ &= \frac{\exp\left\{-bt + \frac{\delta at}{1-2at}\right\}}{(1-2at)^{\frac{n}{2}}}, \end{aligned} \quad (\text{A-3})$$

for  $t < \frac{1}{2a}$ . Define  $\phi(t)$  as the natural logarithm of  $M(t)$ ,

$$\phi(t) = -tb + \frac{\delta at}{1-2at} - \frac{n}{2} \log(1-2at). \quad (\text{A-4})$$

The derivative of  $\phi(t)$  may be shown to be

$$\phi'(t) = \frac{a(n+\delta) - 4a^2t}{(1-2at)^2} - b. \quad (\text{A-5})$$

It may also be shown that  $\phi''(t) > 0$  for all  $t < \frac{1}{2a}$ , so  $\phi(t)$  is convex. Clearly,  $t = 0$  is a root of  $\phi(t)$ . The other root ( $t^*$ ), which is the nonzero MGF unity root, is negative ( $t^* < 0$ ) when the mean of  $g$ ,

$$\begin{aligned} E[g(Y)] &= aE\{Y\} - b \\ &= a(n+\delta) - b, \end{aligned} \quad (\text{A-6})$$

is positive and positive ( $t^* > 0$ ) when the mean is negative. Thus,  $\phi(t)$  may look like the curves found in figure A-1.

The suggested approach to finding the root  $t^*$  is to find the minimum point of  $\phi(t)$ , move slightly to the left if  $t^* < 0$  or slightly toward  $\frac{1}{2a}$  if  $t^* > 0$  and apply the Newton-Raphson iteration for root finding which has the update equation

$$t_{k+1}^* = t_k^* - \frac{\phi(t_k^*)}{\phi'(t_k^*)}. \quad (\text{A-7})$$

Termination of the update should occur when successive updates of  $t^*$  and  $\phi(t^*)$  fail to change significantly.

The minimum point of  $\phi(t)$  occurs when  $\phi'(t) = 0$ . This results in requiring

$$t^2 + \left(\frac{a-b}{ab}\right)t + \frac{b-a(n+\delta)}{4a^2b} = 0 \quad (\text{A-8})$$

which occurs when

$$t = t_{\pm} = \frac{1}{2a} - \frac{1 \mp \sqrt{1 + (n-2+\delta)\frac{b}{a}}}{2b}. \quad (\text{A-9})$$

If  $n \geq 2$  or  $n = 1$  and  $\delta \geq 1$ , the argument of the square root in equation (A-9)  $> 1$ . Thus, since valid solutions require  $t < \frac{1}{2a}$ , the minimum point in this case is

$$t_+ = \frac{1}{2a} - \frac{1 + \sqrt{1 + (n-2+\delta)\frac{b}{a}}}{2b}. \quad (\text{A-10})$$

For the case of  $n = 1$  and  $0 \leq \delta < 1$ , both roots should be computed and the real one with the correct sign chosen.

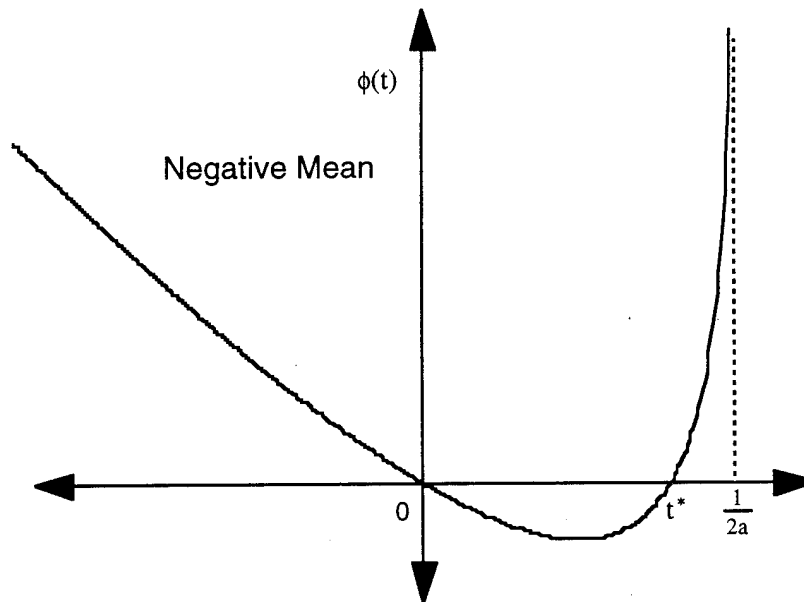
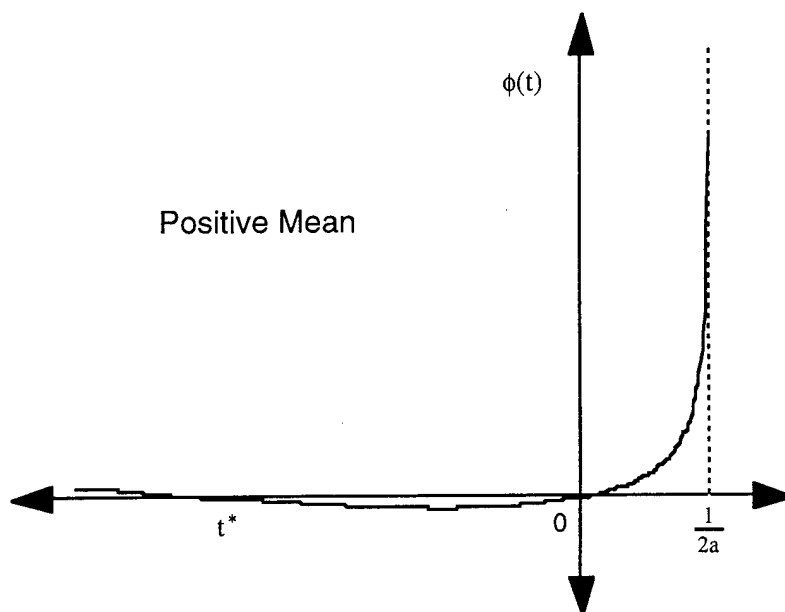


Figure A-1. Possible Configurations of  $\phi(t)$  for Noncentral Chi-squared Random Variable

## INITIAL DISTRIBUTION LIST

Addressee	No. of Copies
Coast Guard Academy (J. Wolcin)	1
Office of Naval Research (Code 451: T. Goldsberry, N. Harned, M. Shipley)	3
Program Executive Office, USW ASTO (J. Polcari)	1
Space and Naval Warfare Systems Command (R. Holland)	1
Naval Undersea Warfare Center, Detachment West Palm Beach (R. Kennedy)	1
Pennsylvania State University (S. Schwartz)	1
University of Connecticut (Y. Bar Shalom, D. Dey, N. Mukhopadhyay, P. Willett)	4
University of Naples (F. Palmieri)	1
University of Rhode Island (D. Tufts)	1
Defense Technical Information Center	12